Appl. Phys. B 68, 211–215 (1999)

Applied Physics B
Lasers
and Optics
© Springer-Verlag 1999

Different temperature dependences of photorefractive parameters of Ce-doped and Rh-doped $BaTiO_3$

M. Chi, S.X. Dou, H. Song, Y. Zhu, P. Ye

Institute of Physics and Center for Condensed Matter Physics, Chinese Academy of Sciences, Beijing 100080, P.R. China
(Fax: +86-10/6256-2605, E-mail: g303@aphy02.iphy.ac.cn)

Received: 16 July 1998/Revised version: 26 October 1998

Abstract. Temperature dependences of the total effective trap density N_{eff} and the electro-optic coefficient r_{33} in Ce-doped and Rh-doped $BaTiO_3$ were determined by two-beam coupling measurements. It was found that the effective trap density N_{eff} of $BaTiO_3$:Ce increases whereas that of $BaTiO_3$:Rh decreases with increasing temperature. The electro-optic coefficient r_{33} of both crystals increases with temperature. The photorefractive response times were also measured and found to decrease with different rates as temperature increases in the two crystals. The results were discussed by using the two-centre model for $BaTiO_3$:Ce and three-charge-state model for $BaTiO_3$:Rh. We found that the different temperature dependence of N_{eff} in the two crystals was due to the fact that the deep- and shallow-trap levels in $BaTiO_3$:Ce are caused by different impurity centres whereas those in $BaTiO_3$:Rh are caused by different charge states of the same impurity centre.

PACS: 42.65.Hw; 42.70.Nq

The photorefractive effect is associated with several properties of photorefractive crystals and usually relies on the crystal temperature. The temperature dependence of the photorefractive effect has been studied in different photorefractive crystals such as $BaTiO_3$ [1, 2], SBN [3, 4], $Bi_{12}GeO_{20}$ [5], and InP [6], and various behaviours of temperature dependence have been observed in these materials. Earlier work [1, 2] on $BaTiO_3$ showed that the photorefractive response time of the crystal always decreases with temperature whereas its two-beam coupling (TBC) gain coefficient may, depending on the samples used, increase or decrease with temperature, resulting, respectively, from an increase or a decrease of the electro-optic coefficients of the crystals. In all these cases, the total effective trap density always decreases with increasing temperature.

During the past several years, Ce-doped and Rh-doped $BaTiO_3$ crystals have been intensively studied in TBC [7, 8] and phase conjugation experiments [9, 10]. It has been found that $BaTiO_3$:Ce and $BaTiO_3$:Rh have improved photorefractive properties compared to undoped crystals in the visible and in the near infrared. Recently, we have investigated the temperature dependence of TBC at a fixed grating period as well as the self-pumped phase conjugation properties of $BaTiO_3$:Ce and $BaTiO_3$:Rh crystals [11, 12], showing that both TBC gain coefficient and speed of response of these crystals can be enhanced at elevated temperature. But the origin of these phenomena in the crystals is not clear.

In this paper, we try to determine how the total effective trap density N_{eff} and electro-optic coefficient of $BaTiO_3$:Ce and $BaTiO_3$:Rh vary with temperature by measuring their TBC coefficient at different grating wave vectors and temperatures. We have found that N_{eff} of $BaTiO_3$:Ce increases with temperature, whereas that of $BaTiO_3$:Rh decreases with temperature. The electro-optic coefficient r_{33} of both samples increases with temperature. In addition, the photorefractive response time of both crystals is found to decrease with temperature in both crystals, though the decrease rates are different. Our experimental results demonstrate that a two-centre photorefractive crystal may have different characteristics of photorefractivity from a three-charge-state crystal.

1 Two-beam coupling theory

In this section we first present the theories that describe the photorefractive effect in Ce-doped and Rh-doped $BaTiO_3$ crystals. These theories will be used in our discussions on the experimental results.

1.1 Two-centre model for $BaTiO_3$*:* Ce

In Ce-doped $BaTiO_3$ crystals, it is already known that there are three impurity levels, a deep one and two shallow ones. These three levels are caused by three different impurity centres [13]. Thus a three-centre model should be used to describe the photorefractive effect in $BaTiO_3$:Ce. But for simplicity we use the two-centre model already well developed [14, 15] to describe the photorefractive effect in $BaTiO_3$:Ce. That is to say, the two shallow-trap levels are regarded as one shallow-trap level. It can be seen later that this

will not affect our discussion. The band diagram of the two-centre model is shown in Fig. 1a where there is a deep level and a shallow level corresponding to the two centres.

In the two-centre model, the electro-optic beam-coupling gain coefficient, γ_{eo}, for hole-dominated photorefractive crystals such as $BaTiO_3$ is given by [14, 15]

$$\gamma_{eo} = \frac{2\pi n^3}{\cos\theta_i}\frac{K_B T}{e}\frac{r_{eff}}{\lambda}\left(\frac{k_g}{1+k_g^2/k_0^2}\right)\eta(I)\left(\hat{\boldsymbol{e}}_1\cdot\hat{\boldsymbol{e}}_2^*\right), \tag{1}$$

where n is the refractive index, θ_i is the internal half angle, K_B is Boltzmann's constant, T is the absolute temperature, r_{eff} is the effective electro-optic coefficient, λ is the wavelength in vacuum, e is the electrical charge, $k_g = 4\pi n\sin\theta_i/\lambda$ is the grating wave vector, k_0 is the Debye screening wave vector. $\eta(I)$ is an intensity-dependent factor, $\hat{\boldsymbol{e}}_1$ and $\hat{\boldsymbol{e}}_2$ are unit vectors along the polarization directions of the two beams.

In (1) k_0 is defined by [14, 15]

$$k_0^2 = \frac{e^2}{\varepsilon k_B T}N_{eff} \equiv \frac{e^2}{\varepsilon k_B T}(N_E + M_E), \tag{2}$$

with

$$N_E = \frac{(N_D - N_F - N_0)(N_F + N_0)}{N_D},$$
$$M_E = \frac{M_0(M_T - M_0)}{M_T}. \tag{3}$$

Here N_E and M_E are, respectively, the intensity-dependent effective deep- and shallow-trap densities. ε is the effective static absolute dielectric constant, N_D is the total deep-trap density, N_F is the uncompensated deep-trap density (i.e., density of deep traps with electrons) at dark. M_T is the total shallow-trap density, $N_0(\approx M_0)$ is the mean density of holes transferred from deep traps to the shallow traps induced by light.

The intensity dependent factor $\eta(I)$ in (1) is defined as

$$\eta(I) = \frac{1}{N_E + M_E}\left(N_E + \frac{M_E}{1+\beta_T/S_T I}\right). \tag{4}$$

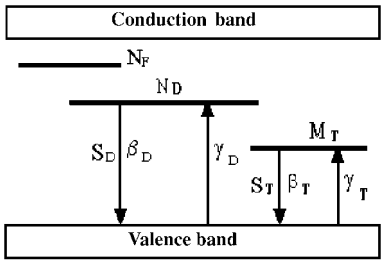

a

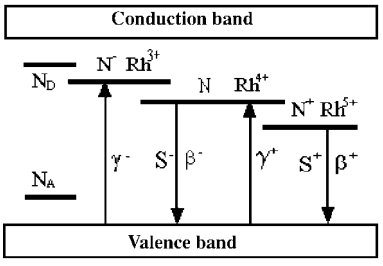

b

Fig. 1a,b. The band diagram of two-center model for $BaTiO_3$:Ce (**a**) and three-charge-state model for $BaTiO_3$:Rh (**b**). Here S, β, and γ represent, respectively, the ionisation cross section, the thermal ionisation rate, and the recombination constant to traps

1.2 Three-charge-state model for $BaTiO_3$*:* Rh

For $BaTiO_3$:Rh crystal, it is already clear that a three-charge-state model should be used to describe its photorefractive effect [16–18]. The band diagram of $BaTiO_3$:Rh is shown in Fig. 1b. It should be noted that as long as the photorefractive charge transfer process is concerned, the three-charge-state levels of Rh can be regarded as a system with a deep-trap level and a shallow-trap level that are related by Rh^{4+}, that is Rh^{3+} and Rh^{4+} together are equivalent to a deep-trap level, and Rh^{4+} and Rh^{5+} together are equivalent to a shallow-trap level. From the following theory, it can be seen that the three-charge-state model has different characteristics from the two-centre model.

In the three-charge-state model, the expression for the electro-optic TBC gain coefficient is the same as that shown in (1). But k_0 and N_{eff} are now defined as [19]

$$k_0^2 = \frac{e^2}{\varepsilon k_B T}N_{eff} \equiv \frac{e^2}{\varepsilon k_B T}\left[N_T - N_0(I_0) - \frac{(N_D - N_A)^2}{N_T}\right], \tag{5}$$

with

$$N_T = N^- + N + N^+, \tag{6}$$
$$N_0 = \frac{1}{1-k}\left\{\left[kN_T^2 + k(k-1)(N_D - N_A)^2\right]^{1/2} - kN_T\right\}, \tag{7}$$
$$k = \frac{S^+ I_0 + \beta^+}{S^- I_0 + \beta^-}\frac{\gamma^-}{4\gamma^+}, \tag{8}$$

where N^-, N, and N^+ are, respectively, the densities of Rh^{3+}, Rh^{4+}, and Rh^{5+}. $N_0(I_0)$ is the mean density of Rh^{4+}, N_D and N_A are the densities of shallow donor and acceptor compensating for the Rh^{3+} and Rh^{5+}.

The intensity-dependent factor $\eta(I)$ in (1) is now defined as

$$\eta(I) = \frac{1}{N_{eff}^+ + N_{eff}^-}\left(N_{eff}^- + \frac{N_{eff}^+}{1+\beta^+/S^+ I}\right), \tag{9}$$

where N_{eff}^+ and N_{eff}^- are intensity-dependent effective trap densities.

It should be pointed out that for the convenience of referring to the original papers [14, 15, 19] about the two theoretical models, we have to use the same symbols to represent different parameters in the theory for the two models.

2 Experiments and results

The $BaTiO_3$:Ce and $BaTiO_3$:Rh crystal samples used in our TBC experiments are normally cut and with dimensions of $a \times b \times c = 1.48\,\text{mm} \times 4.62\,\text{mm} \times 5.40\,\text{mm}$ and $1.26\,\text{mm} \times 6.47\,\text{mm} \times 6.59\,\text{mm}$, respectively. The Ce concentration of the $BaTiO_3$:Ce crystal is 43 ppm and the Rh concentration of the $BaTiO_3$:Rh crystal is less than 10 ppm. The two crystals were grown with an improved top-seeded solution growth technique.

A He-Ne laser at 632.8 nm was used as the light source. The pump and probe beams are *e*-polarized beams with a pump-to-probe intensity ratio of about 400. The intensity of the pump beam is $100\,\text{mW/cm}^2$. The two beams were symmetrically incident on an *a*-face of the crystals. The crystal temperature was controlled by using a Peltier temperature-control device which has a long-term temperature-control stability of less than 0.5 °C. The experimentally determined grating-wave-vector dependence of TBC gain coefficient of the two crystals is shown in Fig. 2.

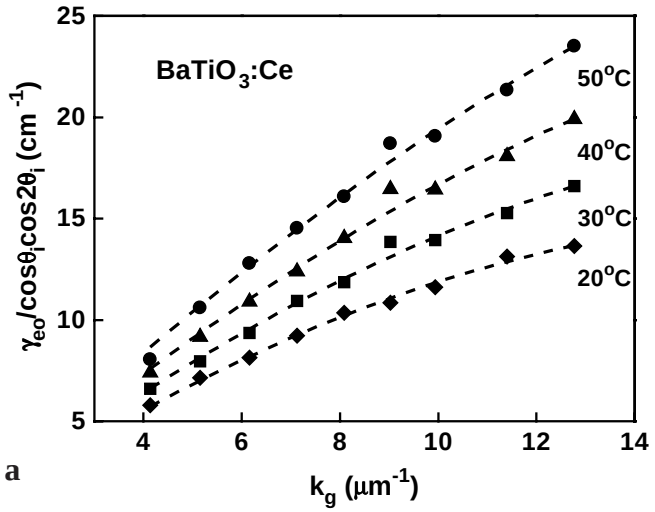

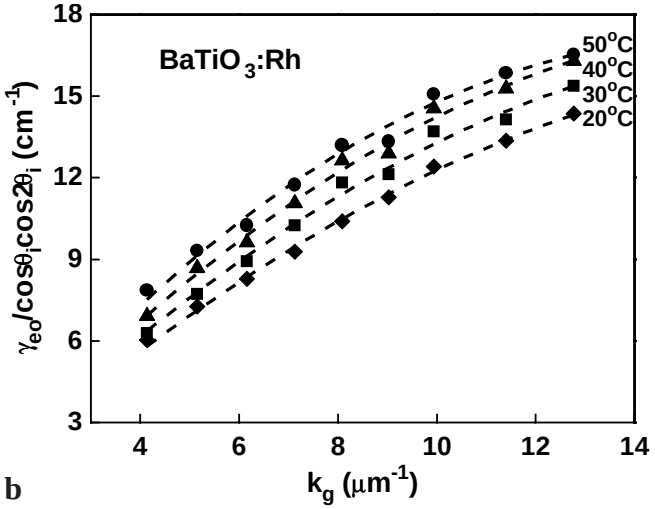

Fig. 2a,b. The TBC gain coefficient as a function of the grating wave vector at different temperatures. **a** $BaTiO_3$:Ce. **b** $BaTiO_3$:Rh. The *curves* are theoretical fits with (1) and (11)

In our present experimental conditions, the term $(\hat{\boldsymbol{e}}_1 \cdot \hat{\boldsymbol{e}}_2^*)$ in (1) is equal to $\cos 2\theta_\text{i}$ and r_eff is [20]

$$r_\text{eff} = \left(-n_0^4 r_{13} \sin^2\theta_\text{i} + n_e^4 r_{33} \cos^2\theta_\text{i}\right)/n_0^3 n_e\,. \tag{10}$$

For $BaTiO_3$ crystals, r_{33} is ~ 3 times larger than r_{13}. In addition, the internal half-angle θ_i in our experiments was less than 15°, thus we have $r_{33}\cos^2\theta_\text{i} \gg r_{13}\sin^2\theta_\text{i}$ and r_eff can be well approximated as

$$r_\text{eff} \approx r_{33}\cos^2\theta_\text{i}\,. \tag{11}$$

By fitting the experimental results at a given temperature with (1) and (11), the total effective trap densities N_eff and $r_{33}\eta(I)$ at that temperature were obtained. The temperature dependences of N_eff and $r_{33}\eta(I)$ thus obtained are presented in Figs. 3 and 4, respectively. It can be seen that N_eff increases

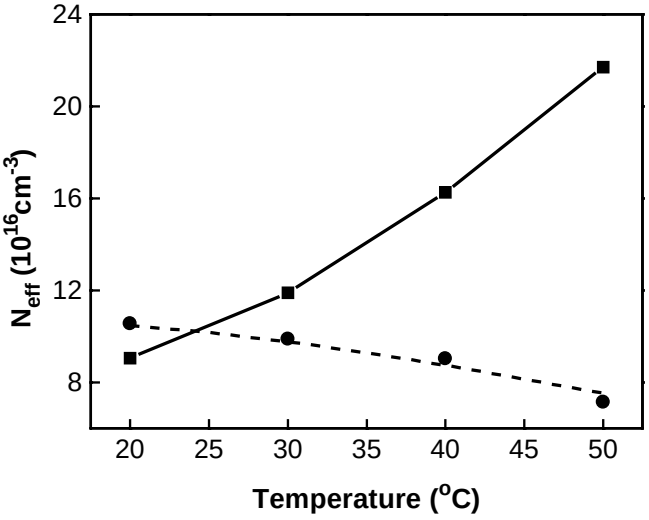

Fig. 3. Total effective trap density of $BaTiO_3$:Ce (*squares*) and $BaTiO_3$:Rh (*circles*) as a function of temperature. The *dashed line* is from theoretical calculation with the parameters given in Table 1

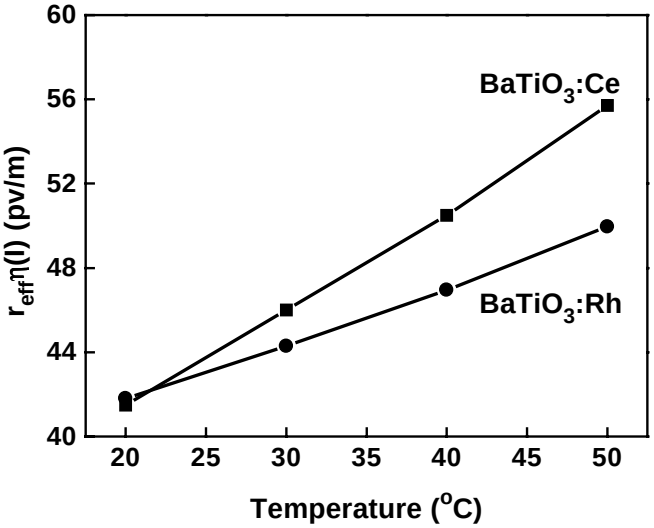

Fig. 4. $r_{33}\eta(I)$ of $BaTiO_3$:Ce and $BaTiO_3$:Rh as a function of temperature

Table 1. The photorefractive parameters used for calculating the total effective trap density in Rh-doped $BaTiO_3$

Parameter	Value
S^+	$2.5\,cm^2/J$ [22]
S^-	$27.5\,cm^2/J$ [22]
β^+	$0.14\,s^{-1}$ at 20 °C [22]
β^-	$\beta^- \ll \beta^+$ [19]
E_A	0.7 eV [22]
γ^-/γ^+	6.0
N_T	$1.53 \times 10^{23}\,m^{-3}$
$N_D - N_A$	$2 \times 10^{21}\,m^{-3}$

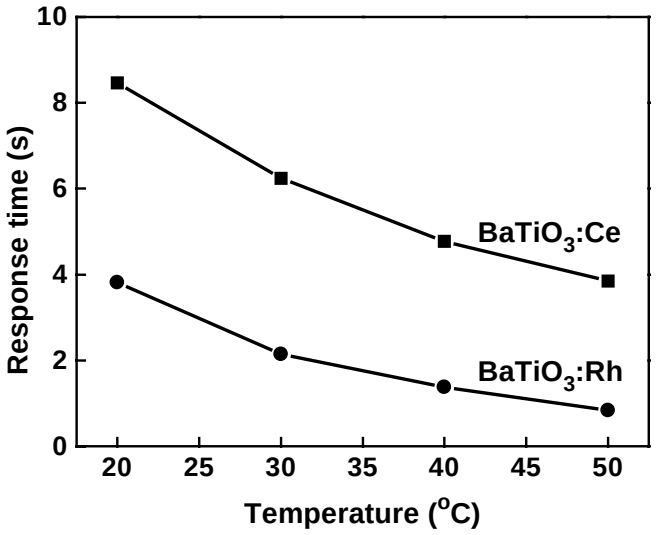

Fig. 5. Temperature dependence of the response time of the two crystals. The erasing intensity is $60\,mW/cm^2$. $\lambda = 632.8$ nm. The grating period is $\Lambda = 0.78\,\mu m$

with temperature in the $BaTiO_3$:Ce crystal, whereas it decreases with temperature in the $BaTiO_3$:Rh crystal. $r_{33}\eta(I)$, however, increases (with different increase rates) with increasing temperature in both crystals. These results will be discussed later.

The photorefractive response time of the crystals at a given temperature has been obtained by recording and fitting (with an exponential decay function) the light-induced decay curves of the diffracted signal of the probe beam while the pump was blocked and the gratings were erased with a third beam. The results are shown in Fig. 5. It can be seen that, in both crystals, the photorefractive response time decreases monotonously with temperature. But the decrease rates are different for the two crystals.

3 Discussion

The different temperature-dependent behaviours of the total effective trap density of the two crystals are interesting. We have measured the light-induced absorption of $BaTiO_3$:Ce and $BaTiO_3$:Rh at different probe wavelengths (the pump light is fixed at 514.5 nm) [13, 21]. We observed that the light-induced absorption of $BaTiO_3$:Ce is negligible when the pump beam intensity is $100\,mW/cm^2$. This means that there are few light-induced holes on the shallow level when the pump intensity is $100\,mW/cm^2$. Considering the fact that the crystal is less absorptive at 632.8 nm than at 514.5 nm, we are certain that the shallow level makes no contribution to the TBC in $BaTiO_3$:Ce in our present experiment at 632.8 nm. In addition, the higher the temperature, the more insignificant the role of the shallow level becomes because of the increasing thermal excitation rate from the shallow-trap levels, β_T. That is to say, we can reasonably regard N_0 in (3) as zero. In this case, we have

$$N_{eff} = N_E = (N_D - N_F)N_F/N_D \approx N_F\,. \tag{12}$$

In obtaining the above approximation, we have made use of the fact that N_F is usually much smaller than N_D in hole-dominated photorefractive crystals such as our $BaTiO_3$:Ce. From the same fact, we can know that the deep level is above the Fermi level in our $BaTiO_3$:Ce. Thus the uncompensated deep trap density at dark, N_F, increases with increasing temperature due to the thermal excitation of electrons from levels that are below and near the Fermi level to the deep level. That is to say, we assume there are some other impurity levels in the crystal where electrons cannot be released with light and usually do not contribute to the photorefractivity of the crystal. This is reasonable because there usually are various transition-metal ion impurities at approximately 1 ppm or even greater in $BaTiO_3$ crystals [15].

Due to the increase of N_F with increasing temperature, we can see from (12) that N_{eff} will increase when the temperature of the crystal is increased. It should be noted that if the light intensity is high and the shallow-trap level becomes involved in the charge transfer process, we expect that N_{eff} will increase less significantly because the density of holes on the shallow-trap levels tends to decrease with increasing temperature. And furthermore, if N_0 is large enough, N_{eff} may become to decrease when the temperature is elevated.

In the case of $BaTiO_3$:Rh, it can be seen from the light-induced absorption experiments that the effect of the shallow level cannot be neglected because the light-induced absorption already saturates at a pump intensity (514.5 nm) of less than $100\,mW/cm^2$ [21]. As the crystal is more absorptive at 632.8 nm than at 514.5 nm, we are certain that the shallow level cannot be neglected in our TBC. In fact, Corner et al. [22] have already observed that light-induced absorption appears when the intensity of the pump at 632.8 nm is as small as $1\,mW/cm^2$. This means that the effective shallow trap density N_{eff}^+ cannot be neglected and it contributes to the total effective trap density. The thermal activation energy E_A of the shallow level $Rh^{4+/5+}$ in $BaTiO_3$:Rh is 0.7 eV [16]. It can be seen from simple calculation that the thermal-excitation rate β^+ of this shallow-trap level increases significantly with temperature. For example, when the temperature rises from 20 °C to 50 °C, β^+ will have a 12-fold increase. Thus as the temperature rises, the effect of shallow level will change significantly. From (5)–(8) it can be seen that the mean density of Rh^{4+}, N_0, will increase with increasing temperature via β^+. This leads to a decrease of N_{eff}.

In order to demonstrate this more clearly, we calculated N_{eff} by using (5)–(8) and the photorefractive parameters as listed in Table 1. The result is given in Fig. 3. It agrees very well with the experimental results. The values of N_T,

$N_D - N_A$, and γ^-/γ^+ as given in Table 1 were chosen to give a good result. But referring to [19, 22], we can see that these values are reasonable. In fact, we found from (5)–(8) that as long as the photoconductivity is great compared with the dark conductivity, i.e., $S^- I_0 \gg \beta^-$, N_{eff} always decreases with increasing temperature. That is to say, it is not possible for N_{eff} to increase in the three-charge-state photorefractive crystals with parameters as listed in Table 1. The reason is that in the three-charge-state $BaTiO_3$:Rh, although N_D (i.e., density of Rh^{3+} at dark) should increase with increasing temperature just like N_F in the two-centre model, the temperature dependence of N_{eff} is mainly decided by that of N_0. But it should be noted that for three-charge-state crystals with parameters that make k in (7) very large, the role of the shallow level will become negligible. In this case, N_{eff} may increase with increasing temperature.

In both $BaTiO_3$:Ce and $BaTiO_3$:Rh, $r_{33}\eta(I)$ increases with temperature. In fact, it has been observed that r_{13} increases with temperature in some $BaTiO_3$ crystals [2, 23]. These results agree with theory, which predicts that r_{13} and r_{33} should increase in the same way with temperature through their proportionality to the temperature-dependent dielectric constant ε_3 of $BaTiO_3$ [3]. In principle, the electro-optic coefficients of $BaTiO_3$ should be independent of the doping elements because the doping concentration is so low that it is far away from affecting the average lattice parameters of the crystal [23]. Thus we believe the different increase rates of $r_{33}\eta(I)$ of $BaTiO_3$:Ce and $BaTiO_3$:Rh should result from different variation behaviours of $\eta(I)$ in the two crystals.

In $BaTiO_3$:Ce, $\eta(I)$ should remain constant, $= 1$, when the temperature varies because of the weak effect of shallow levels (i.e., M_E in (4) is $M_E \approx 0$). Thus the variation of r_{33} of $BaTiO_3$:Ce (also that of $BaTiO_3$:Rh) is equivalent to that of $r_{33}\eta(I)$ for $BaTiO_3$:Ce given in Fig. 4. But in $BaTiO_3$:Rh, the light-induced absorption is almost saturated at $100\,\text{mW/cm}^2$ at room temperature. This means that $\beta^+/S^+ I \ll 1$, and $\eta(I)$ as given in (9) also approaches 1 at room temperature. As the temperature rises, however, β^+ will increase. Thus $\eta(I)$ decreases. This is why the increase rate of $r_{33}\eta(I)$ for $BaTiO_3$:Rh is less than that for $BaTiO_3$:Ce.

From Fig. 5 it can be seen that when the temperature of the crystals rises from 20 °C to 50 °C, the response time of $BaTiO_3$:Ce is decreased by 54% whereas that of $BaTiO_3$:Rh is by 78%. For large grating periods, the response time can be approximated by the dielectric relaxation time $\tau_d \propto \varepsilon N_{\text{eff}}/\mu$ [2]. Here μ and ε are, respectively, the mobility of holes and the dielectric constant along the direction of charge migration (i.e., $\varepsilon = \varepsilon_3$). As the temperature increases, N_{eff} and ε of $BaTiO_3$:Ce increase. Thus the measured decrease of response time implies that the mobility μ increases with temperature significantly. This has been observed in other crystals [24]. In $BaTiO_3$:Rh, the variation of N_{eff} is different from that in $BaTiO_3$:Ce, i.e., it decreases with temperature. The other two parameters, ε and μ, however, should have the similar behaviours in the two crystals. Thus the response time of $BaTiO_3$:Rh decreases more significantly than that of $BaTiO_3$:Ce.

4 Conclusion

We have determined the temperature dependence of the total effective trap density N_{eff} and the electro-optic coefficient r_{33} of $BaTiO_3$:Ce and $BaTiO_3$:Rh by measuring their TBC gain coefficients at different grating periods and crystal temperatures. We have found the temperature dependences of N_{eff} of the two crystals are different: N_{eff} increases with temperature in $BaTiO_3$:Ce and decreases in $BaTiO_3$:Rh. We have also observed that, in both crystals, $r_{33}\eta(I)$ increases, and the response time decreases with increasing temperature. But the increase rates as well as the decrease rates are different in the two crystals. Some of the results were discussed qualitatively with theories of the two-centre model and three-charge-state models. Our study demonstrates clearly that two-centre crystals and three-charge-state crystals may be similar in some of their photorefractive properties, but may be different in their other photorefractive properties.

Acknowledgements. We thank the reviewers for their helpful suggestions. This research was supported by a grant for key research projects in the Climbing Program from the State Science and Technology Commission of China, and also by the National Natural Science Foundation of China.

References

1. S. Ducharme, J. Feinberg: J. Appl. Phys. **56**, 839 (1984)
2. D. Rytz, M.B. Klein, R.A. Mullen, R.N. Schwartz, G.C. Valley, B.A. Wechsler: Appl. Phys. Lett. **52**, 1759 (1988)
3. D. Rytz, B.A. Wechsler, R.N. Schwartz, C.C. Nelson, C.D. Brandle, A.J. Valentino, G.W. Berkstresser: J. Appl. Phys. **66**, 1920 (1989)
4. K. Sayano, G.A. Rakuljic, A. Agranat, A. Yariv, R.R. Neurgaonkar: Opt. Lett. **14**, 459 (1989)
5. I. Foldvari, J.J. Martin, C.A. Hunt, R.C. Powell, R.J. Reeves, A. Peter: J. Appl. Phys. **74**, 783 (1993)
6. C. Özkul, S. Jamet, V. Dupray: J. Opt. Soc. Am. B **14**, 2895 (1997)
7. C. Yang, Y. Zhang, P. Yeh, Y. Zhu, X. Wu: Opt. Commun. **113**, 416 (1995)
8. M. Kaczmarek, R.W. Eason: Opt. Lett. **20**, 1850 (1995)
9. S.X. Dou, H. Gao, J. Zhang, Y. Lian, H. Wang, Y. Zhu, X. Wu, C. Yang, P. Ye: J. Opt. Soc. Am. B **12**, 1048 (1995)
10. A. Brignon, J.-P. Huignard, M.H. Garrett, I. Mnushkina: Opt. Lett. **22**, 215 (1997)
11. S.X. Dou, Y. Ding, H.J. Eichler, Y. Zhu, P. Ye: Opt. Commun. **131**, 322 (1996)
12. M. Chi, S.X. Dou, H. Gao, H. Song, J. Zu, Y. Zhu, P. Ye: Chin. Phys. Lett. **14**, 838 (1997)
13. H. Song, S.X. Dou, M. Chi, H. Gao, Y. Zhu, P. Ye: J. Opt. Soc. Am. B **15**, 1850 (1998)
14. P. Tayebati, D. Mahgerefteh: J. Opt. Soc. Am. B **8**, 1053 (1991)
15. M.H. Garrett, J.Y. Chang, H.P. Jenssen, C. Warde: J. Opt. Soc. Am. B **9**, 1407 (1992)
16. H. Kröse, R. Scharfschwerdt, O.F. Schirmer, H. Hesse: Appl. Phys. B **61**, 1 (1995)
17. K. Buse: Appl. Phys. B **64**, 273 (1997)
18. K. Buse, E. Krätzig: Appl. Phys. B **61**, 27 (1995)
19. N. Huot, J.M.C. Jonathan, G. Roosen: Appl. Phys. B **65**, 489 (1997)
20. J. Zhang, Y. Lian, S.X. Dou, P. Ye: Opt. Commun. **110**, 631 (1994)
21. H. Song, S.X. Dou, M. Chi, H. Gao, Y. Zhu, P. Ye: J. Opt. Soc. Am. B **15**, 1329 (1998)
22. L. Corner, R. Ramos-Garcia, A. Petris, M.J. Damzen: Opt. Commun. **143**, 165 (1997)
23. P. Bernasconi, M. Zgonik, P. Günter: J. Appl. Phys. **78**, 2651 (1995)
24. P. Nouchi, J.P. Partanen, R.W. Hellwarth: J. Opt. Soc. Am. B **9**, 1428 (1992)